ISSN (Print) 2794-7629 Received 18/02/2025
ISSN (Online) 2794- 4549 Accepted 12/03/2025

**FULL PAPER**

# The Ideal Distance for Determining the Size of a Huge Air Shower at High Energies

***Prepared by***

***Abbas Rahi Raham***
*Directorate General of Education Babylon*
*abbasrahi750@gmail.com.*
*0000-0002-7130-6934*

**Abstract**

To determine the size of the air shower, we must have a more accurate knowledge that describes the fall of the signal size from the core of the shower, i.e. its lateral distribution**.** In this work, the lateral distribution ($S_{38}$) within the range of energies (*1-10 EeV*) of the nuclei of elementary iron atoms and protons and a mixture of proton particle and nuclei of iron atoms which is proportional to the signal S(r) with the primary energy were studied. "We estimate the distribution function at (1000 m) from the core of the particle interaction within the energy range and zenith angles of ($30^o$- $60^o$). The distribution of the signal *S* (*r*) for a barrage of charged particles such as protons, iron nuclei and a mixture of a proton particle and iron nuclei was calculated on the range of distance from the axis of interaction of particles (*200-4000 m*) using the (MATLAB) program for different initial energies. The experimental measurements and the theoretical outcomes were contrasted of the proton and iron nuclei in good agreement in the energy range of" (*1-10EeV*).

**Keywords:** Extensive air showers, Cosmic rays, Lateral distribution function, Knee

## Introduction

Cosmic rays do not reach the earth directly because they go through a series of nuclear reactions in the atmosphere. Particles produced from elementary reactions undergo further interactions. Ever since the extensive air showers were discovered in the late 1930s, it became clear that the origin of high-energy cosmic rays was remains elusive, but it remains a big mystery to this day. [2,3,13,19,20].The largest cosmic ray record event is the one recorded by John Linsey in 1962 with an energy of $10^{20}$ eV [16]. Through subsequent studies, nearby levels are above $10^{20}$ eV [1,4,14,21]. The energy spectrum and chemical makeup can provide insights into cosmic ray acceleration and propagation, which are the two most significant processes that move the particles in the universe [11,17]. A single high-energy primary CR interacts with atmospheric nuclei to produce Extensive air showers. Many secondary charged particles are the end product of this interaction. Higher energy cosmic rays, however, have a significantly smaller flux and must be detected by the $EAS_s$ that are created when CRs interact with atmospheric molecules [6]. A simple model developed by Heitler that depicts it is possible to identify the essential features of a pure electromagnetic cascade formation by examining its progression in $EAS_s$ [22]. The lateral distribution function of particles (LDF) is a crucial tool for studying the high energy of $EAS_s$.For primary protons, iron nuclei, and mixed particles (defined as an equal part combination of iron and proton 50:50) for the energies (0.1, 1and 10) EeV at various zenith angles, the LDF was calculated at a distance of 1000m from the shower axis, S(1000m).There was good agreement between the measurements and the LDF derived findings.

## Discrete-Time Distribution Model

An effective method for examining spectral changes in the atmosphere is to use the Lateral Distribution Function (LDF) of particles, S(1000m). The signal in VEM units that would be generated in a tank 1000 m away from the shower axis is the parameter S(1000m), which describes the energy of a cosmic ray shower that was picked up by the SD array. At the core distance of 1000 m, the LDF of particles, S(1000m), which depends on the zenith angle and the original primary particle's energy $E_o$ [15]. Given the direct relationship between S(1000m) and this number, the shower impact point needs to be precisely determined. It was discovered that a modified NKG function and a power-law-like function provide the best description [7]. An NKG function that has been slightly altered was employed in this analysis:

$$f_{LDF}(r) = \left(\frac{r}{r_{1000}}\right)^{-\beta} \left(\frac{r+r_{700}}{r_{1000}+r_{700}}\right)^{-\beta} \qquad 1$$

With r700 = 700m; r1000= 1000m and the slope β fixed according to the following parameterization [12]:

$$\beta(\theta) = \begin{cases} a + b(sec\theta - 1), & sec\theta < 1.55\ (\theta \geq 50^o) \\ a + b(sec\theta - 1) + f(\sec\theta - 1.55)^2, & sec\theta \geq 1.55 \end{cases} \qquad 2$$

With: $a = 2.26 + 0.195loge\ ;\ b = -0.98,$

$$c = 0.37 - 0.51sec\theta + 0.30sec^2\theta\ ; e = c(S1000)^d, \qquad 3$$

$$d = 1.27 - 0.27sec\theta + 0.08sec^2\theta\ ; f = -0.29.$$

A realistic *S(1000)* of the event could be obtained from [18]**:**

$$S(1000)(\theta) = S_{38} \times [1 + Cx - Dx^2] \qquad 4$$

$$S_{38} = \left(\frac{E}{A}\right)^{1/B} [VEM] \qquad 5$$

This is driven by the necessity to examine the distinction between fitting a power law function, which assumes Gaussian uncertainty on *E* and $S_{38}$, and fitting a linear function, which is equal to assuming log-normal uncertainties for these variables. In this regard, the information is not definitive. Another exponential function for *S*(*1000m*) can be obtained with the form [12]:

$$S(1000) = S_{38}\ exp[X_O/\lambda(sec\,\theta - sec\,\theta_{38})] \qquad 6$$

Where λ=-934 g/cm2 is the splitting length and $X_o$=879 g/cm2 is the atmosphere's total vertical depth.

**Table.1.** the Coefficients *A*, *B*, *a* and *b* for primary protons, Iron nuclei and mixed particles [12].

| | ***Iron*** | ***Proton*** | ***Mixed*** |
|---|---|---|---|
| *A* | 0.208 | 0.239 | 0.218 |
| *B* | 1.074 | 1.069 | 1.071 |
| *a* | 1.19 | 1.12 | 1.19 |
| *b* | -1.11 | -1.78 | -1.53 |

Assuming a real LDF, the signal gathered at each station during a certain shower with a specified energy and zenith angle is set [18]. Acquired by Kamata and Nishimura, and then calculated by Greisen in the famous NKG formula, one can gets [5,9]**:**

$$S(r) = S(1000m)\left(\frac{r}{r_{1000}}\right)^{-\beta}\left(\frac{r+r_{700}}{r_{1000}+r_{700}}\right)^{-\beta} \quad 7$$

**Results and Discussions**

In figure 1. For primary iron nuclei, proton, and mixed particles, the lateral distribution at zenith angles 38$^{o}$ at the energy range (1–10EeV) is visible, demonstrating that the signal $S_{38}$ is proportional to the primary energy.

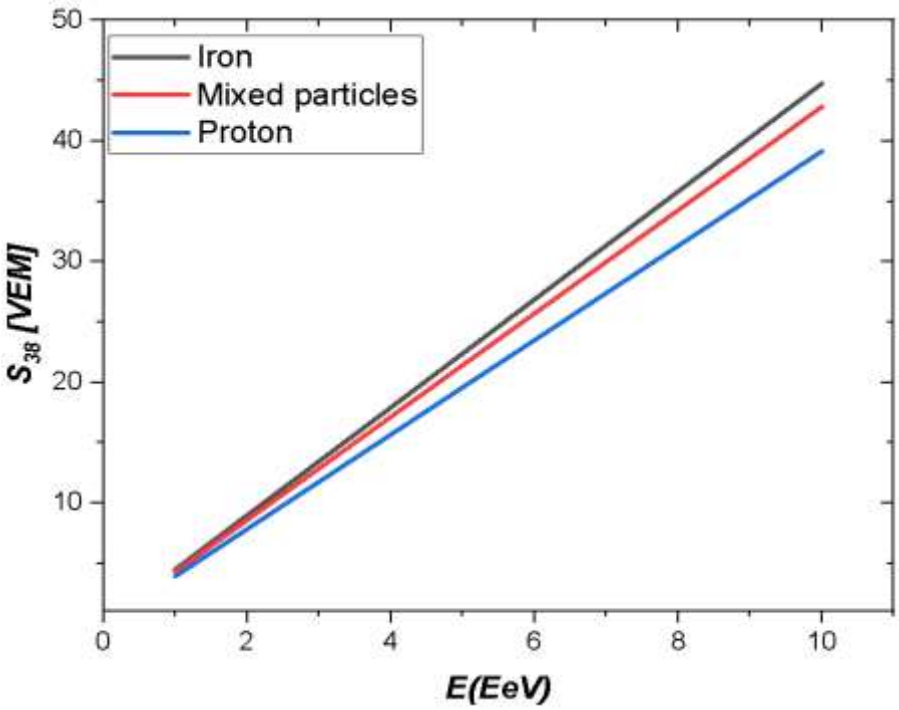



Fig. 1. Eq. (5) and table (1) are used to calculate $S_{38}$ for iron nuclei, protons, and mixed particles at energies between 1 and 10 EeV.

Figure.2. demonstrates that S(1000) is dependent on the zenith angle and the primary energy of cosmic rays with an energy range of 1014–1019 eV. Eq. (6), which depends on S38 for various zenith angles (0o, 45o, and 60o), shows that S(1000) grows with primary energy for each particle, such as protons, in this image. Vertical component of the shower curve for S(1000) is higher than that for slant angles (45o and 60o), as can be seen from this figure.

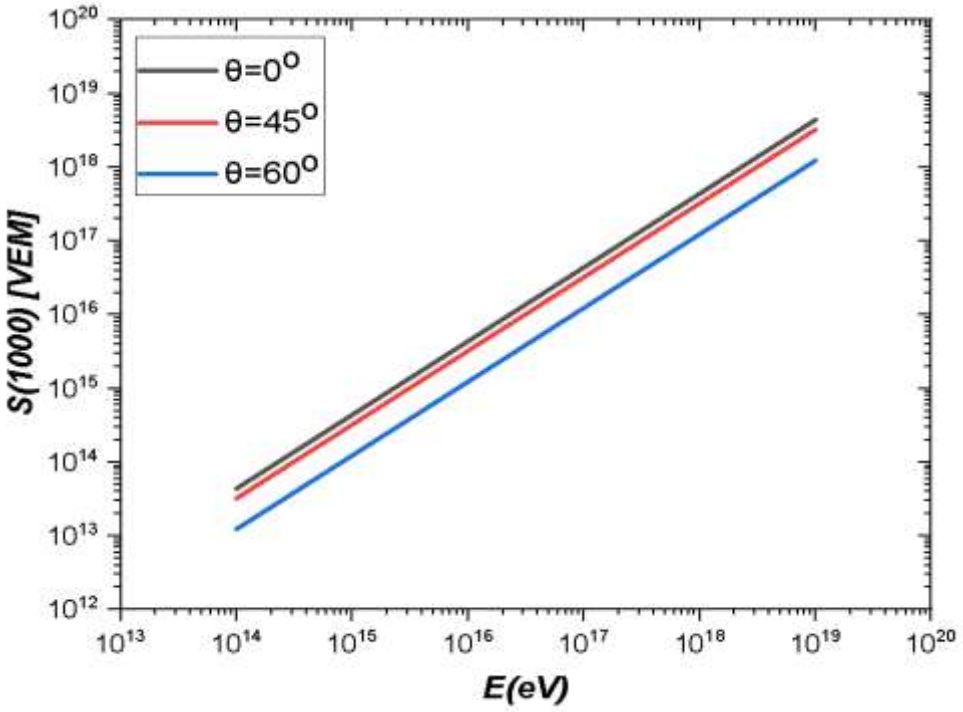



Fig. 2. Eq. (6), for primary protons and various angles (1) 0o (2) 45o (3) 60o, is used to calculate S1000 at the primary energy range between 1014 and 1019eV.

Figure.3. displays the findings of the EAS calculation for the energy EeV at 10 with various angles (30o-60o) and the S(1000) polynomial function, which was started by primary protons, iron, and mixed particles. The geometrical effects and shower attenuation cause S(1000) to drop with zenith angle. This is because, from the perspective of the shower front, the array spacing appears smaller at large angles, which causes S(1000) to decrease.

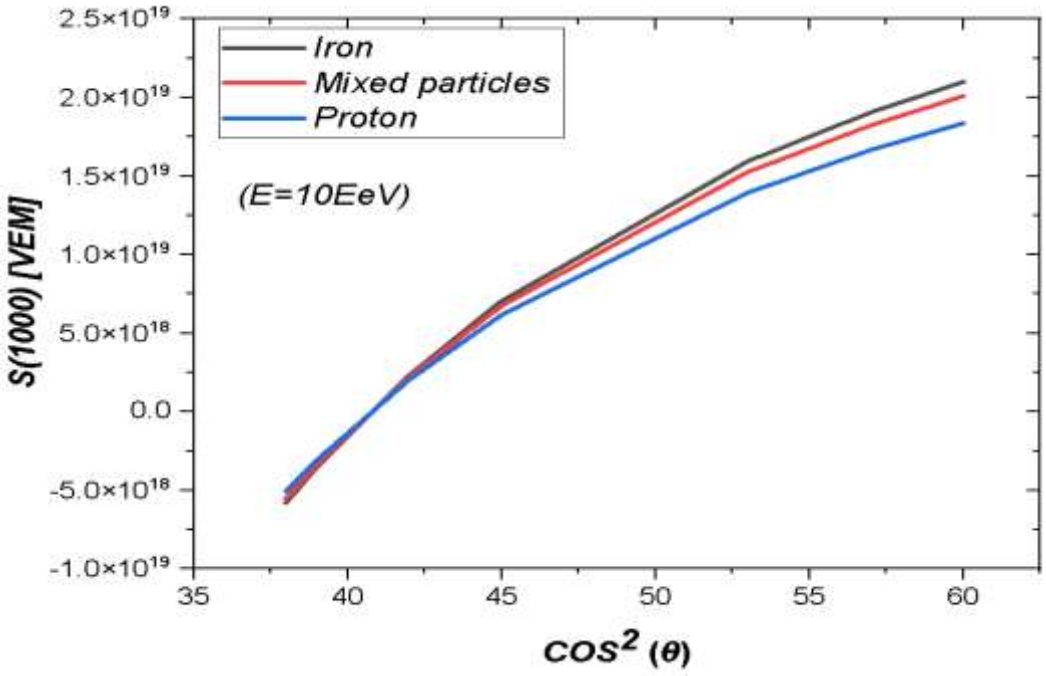



Fig. 3. Eq. (4) and table (1) for primary protons, iron, and mixed particles along with angles between 30o and 60o degrees are used to calculate the polynomial function (S1000) at the primary energy of 10EeV.

Figure (4) displays the findings of the EAS calculation for energy 1EeV in the zenith angle range of 30o to 60o and S(1000) exponential function, which was started by primary protons, iron nuclei, and mixed particles. The type of primary particles and the shower's zenith angle determine S(1000) in this figure.

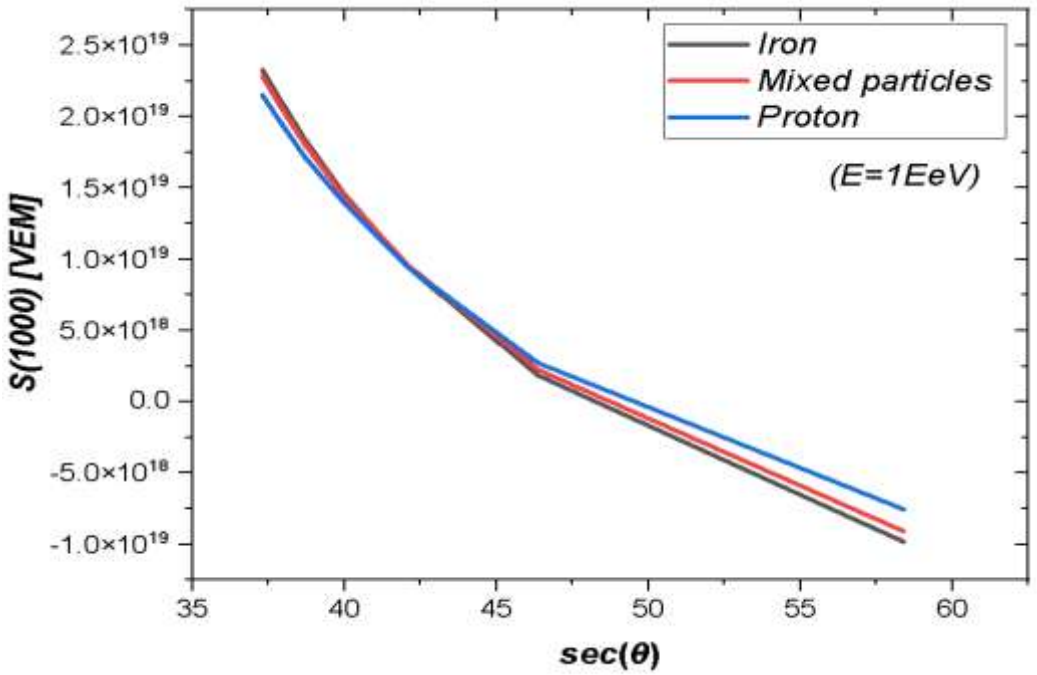


Fig. 4. For main protons, iron nuclei, and mixed particle, the exponential function (S1000) at primary energy 10 *EeV* is calculated using Eq. (6) and table (1), with angles ranging from 30o to 60o.

Figure (5 ) shows the results of the calculation for EAS triggered by iron nuclei, mixed particles, and primary protons for S(r) at energy 10EeV and zenith angle range 30o-60o at distances between 400 and 4000m from the shower axis. This picture illustrates how S(r) is dependent on both the primary energy and the distance from the shower axis.

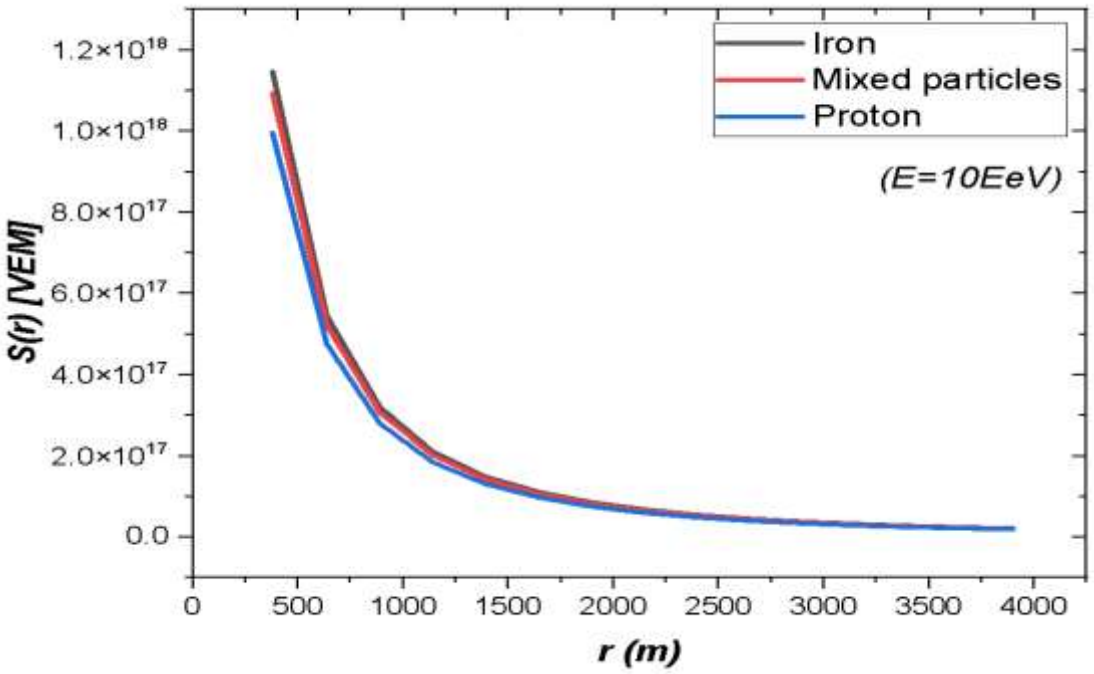



Fig.5. Eq (7) and table (1) for main protons, iron nuclei, and mixed particles at various angles (30o-60o) are used to calculate S(r) for the primary energy 10EeVat at the distance from a shower axis (r) range (400-4000m).

Figure 6. Illustrates how particles with high energy behave in ambiance at energies ranging from 1014 to 1019 eV, for primary protons at various angles (0o, 45o, and 60o) at a distance of 1000 m from the shower axis. It also demonstrates that *S(r)* is dependent on both the main energy and the zenith angle.

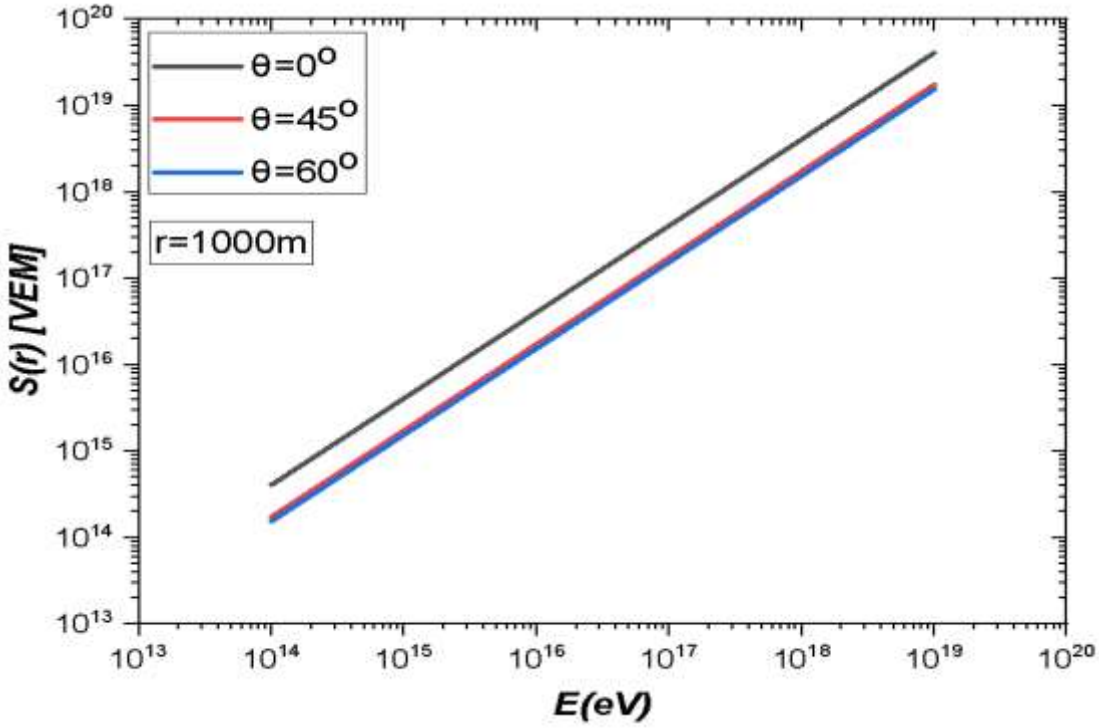



Fig.6. For the distance from the shower axis (r = 1000), S(r) at the primary energy range between 1014 and 1019eV is calculated using Eq. (7) for primary protons and various angles (1) 0o (2) 45o (3) 60o.

In Figure 7, the experimental results [8, 10] with theoretical data shown a good fit between the two proton and an elementary iron nuclei inside the energy between (1-10EeV) at different zenith angles.

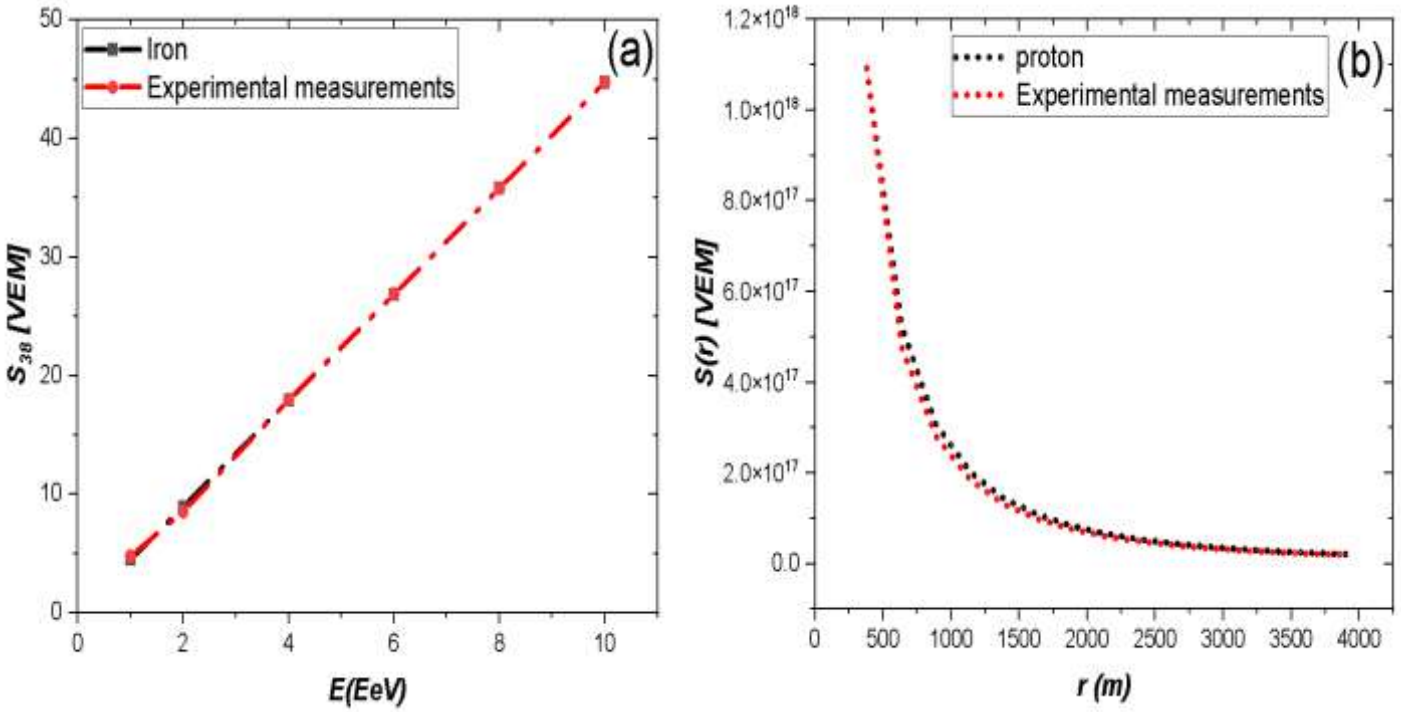



Fig. 7. Presents the experimental results [8,10] of the proton and iron nuclei with respect to the primary energies and its contrasting the energy range with the theoretical data (1-10EeV) :- (A): The lateral distribution at zenith angles $38^{o}$ for iron nuclei shows that the $S_{38}$ signal is proportional to the initial energy. (b): The signal station S(r) of the EAS initiated by the proton at energy 10 and zenith angles within ($30^{o}$-$60^{o}$) away from the axis of the shower.

As shown in Figure 1, the majority of active in this study, the event's energy is 10EeV, which shows the signal $S_{38}$ according to the initial energy of a lateral distribution of the iron nucleus greater than the rest of the particles at zenith angles $38^{o}$. In Figure 2, we find that S(1000) depends mainly on the zenith angles and the initial energy of cosmic rays in the energy range 1014-1019 eV. The vertical Shower curve S(1000) is higher than the oblique angles ($45^{o}$-$60^{o}$). In Figure (3.4), the attenuation of the shower and the geometric effects lead to a decrease in S(1000) at zenith angles, because from the perspective of the front of the shower, the array spacing appears smaller at large angles, which leads to a decrease in S(1000). In Figure (5.6) the dependence of S(r) on the primary energy, peak angles and distance from the shower axis within the range of (400-4000 m). Figure 7 Experimental measurements [8, 10] with theoretical evidence demonstrating a satisfactory compatibility of A: Iron and b: proton in the range of energies mentioned higher up.

**Conclusion**

When calculating the lateral distribution function of particles at (1000 m), the work becomes distinct in the stages of growth of the atmospheric shower of the elementary protons as well as the nuclei of iron atoms and mixed particles (proton and iron nuclei) at large levels of energy, in order to know the general characteristics of the lateral evolution of the shower and observe the collective effect on this development, we increase the different peak angles in the range ($30^{o}$-$60^{o}$)to analyze the different

secondary side distributions. When reconstructing elementary particle parameters, it depends on the timing of the geometry and on the distribution of signal densities as a function of the lateral distance of the shower axis and the energy. S(r) for elementary protons and iron nucleus at a distance from the Shower axis range (400-4000 m) and within the range of the mentioned angles, "This was calculated using approximated lateral energy functions" that showed good particle compatibility. Basic samples for the analysis of air shower lateral events recorded and observed in important and enormous shower arrays are part of current studies.

**References**

[1] Afanasiev, B., Dyakonov, M. N., Egorov, T. A., Egorova, V. P., & Efremov, N. N. (1993). Recent results from Yakutsk experiment. In Proceedings of the Tokyo Workshop on Techniques for the Study of the Extremely High Energy Cosmic Rays, Institute for Cosmic Ray Research, University of Tokyo, Tokyo, Japan (p. 35).

[2]Auger, P., Ehrenfest, P., Maze, R., Daudin, J., & Fréon, R. A. (1939). Extensive cosmic-ray showers. Reviews of modern physics, 11(3-4), 288.

[3]Auger, P., Maze, R., & Robley, A. F. (1939). Extension et pouvoir pénétrant des grandes gerbes de rayons cosmiques. Comptes rendus, 208, 1641.

[4] Bird, D. J., Corbato, S. C., Dai, H. Y., Elbert, J. W., Green, K. D., Huang, M. A., ... & Thomas, S. B. (1995). Detection of a cosmic ray with measured energy well beyond the expected spectral cutoff due to cosmic microwave radiation. Astrophysical Journal, Part 1 (ISSN 0004-637X), vol. 441, no. 1, p. 144-150, 441, 144-150.

[5] BuiDuc Hieu.(2005).Ph.D. Thesis University of Leeds.

[6] David Scott Barnhill.(2005) (2008). Ph.D. Thesis, University of California Los Angeles.

[7] David William Newton. (2005).Ph.D.Thesis University of Leeds.

[8] Dova, M. T., Martínez, N., Mariazzi, A. G., Wahlberg, H. P., & Pierre Auger Collaboration. (2015). The Pierre Auger Cosmic Ray Observatory. Nuclear Instruments and Methods in Physics Research A, 798.

[9] Gámez, D. G. (2010). Muon Arrival Time distributions and its relationship to the mass composition of Ultra High Energy Cosmic Rays: An application to the Pierre Auger Observatory (Doctoral dissertation, Universidad de Granada).

[10] Góra, D. (2024). Muon measurements at the Pierre Auger Observatory. SciPost Physics Proceedings, (15), 020.

[11] Hörandel, J. R. (2004). Models of the knee in the energy spectrum of cosmic rays. Astroparticle Physics, 21(3), 241-265.

[12] Ioana Codrina Mari.(2008).Ph.D. Thesis University of Karlsruhe.

[13] Kolhörster, W., Matthes, I., & Weber, E. (1938). Gekoppelte Höhenstrahlen. Naturwissenschaften, 26(35), 576-576.

[14] Lawrence, M. A., Reid, R. J. O., & Watson, A. A. (1991). The cosmic ray energy spectrum above 4* 1017 eV as measured by the Haverah Park array. Journal of Physics G: nuclear and particle physics, 17(5), 733.

[15] Letessier-Selvon, A., & Stanev, T. (2011). Ultrahigh energy cosmic rays. Reviews of modern physics, 83(3), 907-942.

[16] Linsley, J. (1963). Evidence for a primary cosmic-ray particle with energy 10 20 eV. Physical Review Letters, 10(4), 146.

[17] Piazzoli, B. D. E., Liu, S. M., Della Volpe, D., Cao, Z., Chiavassa, A., Guo, Y. Q., ... & Zhu, H. (2022). Cosmic-Ray Physics. Chinese Physics C, 46(3), 030004.

[18] Ros, G., Medina-Tanco, G. A., Supanitsky, A. D., Del Peral, L., & Rodriguez-Frias, M. D. (2011). Energy and Xmax reconstruction of hadron-initiated showers in surface arrays. arXiv preprint arXiv:1110.1179..

[19] Rossi, B. (1934). I risultati della Missione scientifica in Eritrea per lo studio della radiazione penetrante (Raggi cosmici). Misure sulla distribuzione angolare di intensita della radiazione penetrante all'Asmara. La Ricerca Scientifica. Supplemento, 1(9-10), 579-589.

[20] Schmeiser, K., & Bothe, W. (1938). Die harten ultrastrahlschauer. Annalen der Physik, 424(1-2), 161-177.

[21] Takeda, M., Sakaki, N., Honda, K., Chikawa, M., Fukushima, M., Hayashida, N., ... & Yoshii, H. (2003). Energy determination in the akeno giant air shower array experiment. Astroparticle Physics, 19(4), 447-462.

[22] Unger, M. (2008). Cosmic rays above the knee. arXiv preprint arXiv:0812.2763